THE JOURNAL OF PHYSICAL CHEMISTRY B

ARTICLE

pubs.acs.org/JPCB

Modeling the Vibrational Dynamics and Nonlinear Infrared Spectra of Coupled Amide I and II Modes in Peptides

Arend G. Dijkstra,[†] Thomas la Cour Jansen, and Jasper Knoester*

Centre for Theoretical Physics and Zernike Institute for Advanced Materials, University of Groningen, Nijenborgh 4, 9747 AG Groningen, The Netherlands

Supporting Information

ABSTRACT: The amide vibrational modes play an important role in energy transport and relaxation in polypeptides and proteins and provide us with spectral markers for structure and structural dynamics of these macromolecules. Here, we present a detailed model to describe the dynamic properties of the amide I and amide II modes and the resulting linear and nonlinear spectra. These two modes have large oscillator strengths, and their mutual coupling plays an important role in their relaxation. Using first-principles calculations of NMA-d_7 and a dipeptide in a fluctuating bath described by molecular dynamics simulations, we model the frequencies of the local vibrations as well as the coupling between them. Both the coherent couplings and the fluctuations induced by contact with their environment are taken into account. We apply the resulting model of interacting fluctuating oscillators to study the collective vibrations and the partially coherent transport of vibrational energy through a model α-helix. We find that the instantaneous vibrations are delocalized over a few (up to four) amide units, while the coherences in the helix survive for 0.5−1 ps, leading to coherent transport on a similar time scale.

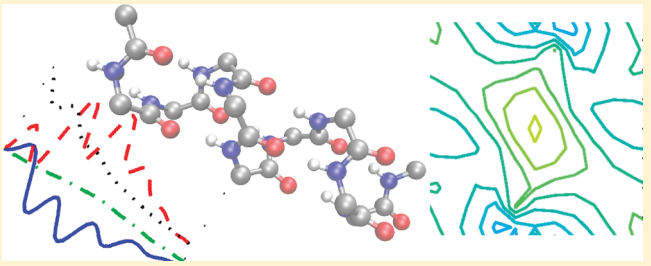

1. INTRODUCTION

Over the past decade, infrared spectroscopy of polypeptides and proteins has developed into a rich field of research, in particular, after the introduction of two-dimensional infrared (2DIR) spectroscopy. The quest is for spectral probes of energy transport and relaxation at femtosecond time scales and for markers of structure and structural dynamics in the two-dimensional spectra.[1,2] In particular, the amide I mode, that is, the vibration of the C═O bond occurring in each amide unit of the polypeptide, is frequently probed in experimental studies. The reason is that this vibration has a strong transition dipole, resulting in easily discerned spectral contributions as well as appreciable interactions between closely separated oscillators, which in turn lead to collective vibrations and sensitivity to structure.

Early 2DIR studies have shown that the amide I vibrations in polypeptides indeed are of a collective nature. In the first report of a 2DIR spectrum of polypeptides, the size of the collective vibrations, defined as the distance over which quantum coherence persists, was found to be 8 Å.[1] This means that a few amide groups are moving with a well-defined phase relation. This observation, in turn, must mean that on this length scale, energy is flowing coherently through the amide I vibrations.

The quantum coherence induced by the electrodynamic and through-bond interactions between local modes on separate amide units is counteracted by interactions with thermally excited low-frequency modes in the solvent and the protein, which cause rapid dephasing and destroy the coherence over large distances. If the coupling to the environment is strong enough, quantum coherent transport will be absent. Therefore, in order to understand the importance of quantum coherence for the energy transport in a protein and its effect on infrared spectra, it is crucial to model the couplings between various amide modes as well as between these modes and the environment. The interaction with the environment also leads to dissipation: an overall loss of energy in the high-frequency mode of interest. The pathways of energy flow in peptides are far from completely known, and several modes have been suggested to accept the energy from an initially excited amide I excitation.[3] Modeling these dynamics is a complex problem because of the large number of degrees of freedom involved. In principle, nonequilibrium MD simulations allow the calculation of the energy flow through all of the vibrational modes in a polypeptide and the solvent.[4] However, because such methods are based on classical equations of motion, they cannot describe coherent energy transfer.

In this study, we will focus on the coupled dynamics of amide I and amide II vibrations and describe this system quantum mechanically, accounting for interactions with a classical solvent. The amide II mode is dominated by the C−N vibration; it is optically weaker than the amide I vibrations and occurs at a frequency that is on the order of 100 cm^{-1} lower. From experimental work[5,6] and our earlier theoretical modeling,[7] confirmed by quantum chemical calculations on *N*-methyl acetamide (NMA)−water

Special Issue: Shaul Mukamel Festschrift

Received: October 1, 2010
Revised: November 30, 2010
Published: January 06, 2011

clusters,[8] we believe that the coupling to amide II vibrations induced by the fluctuating environment is one of the most important decay channels for amide I excitations.

The method presented by us is an extension of the quantum mechanical oscillator approach that was introduced to analyze the amide I spectrum of peptides and proteins. In its first form, it used a transition dipole coupling model to describe the coupling between different amide I units, and a Ramachandran-angle-dependent ab initio map was used for the nearest-neighbor coupling.[9] Electrostatic maps based on ab initio calculations were established to connect the amide I frequency to the electrostatic potential or field generated by the surrounding peptide and solvent environment.[10−16] Recently, an empirical mapping was proposed as well.[17] Improved long-distance coupling methods such as the transition charge coupling scheme have been developed.[18,19] These mappings have been applied successfully to the interpretation of the amide I band absorption and 2DIR spectra of peptides and proteins.[20−27] Although these maps have been successful in explaining the spectral properties of the amide I modes as seen in experiments, vibrational relaxation — energy flowing away from the amide I modes — has hardly been explored.

Recently, experimental attention has been directed toward the amide II band and, in particular, to the cross peaks between the amide I and amide II bands observed in the 2DIR spectra.[5,28] The cross peaks were found to contain structural information. To simulate these types of experiments and model the relaxation from amide I to amide II modes or vice versa, one needs not only to know how the amide I oscillator frequency depends on the state of the environment, but this information is also needed for the amide II frequency, as well as the couplings between various amide I and II modes. A few frequency maps have been proposed,[12,29,30] and nearest-neighbor maps for the couplings were developed[28,31] using matrix reconstruction[32] or discrete differentiation of potential energy surfaces. It turns out that the amide II vibration is very sensitive to the deuteration of the carbon atoms in the NMA molecule used to obtain the maps.

As it is our aim to apply the model to polypeptides, we have chosen to develop a new parametrization that uses fully deuterated carbon atoms (NMA-d_7) in order to describe the response of the oscillator frequency to its environment. The reason is that in this isotope, the methyl umbrella groups contribute less to the vibrational eigenmodes than in the nondeuterated form. This is an essential property because these methyl groups do not exist in the polypeptides. The couplings between vibrations in nearest-neighbor amide groups in the polypeptide are modeled using a mapping derived from ab initio calculations on a dipeptide. Some results employing our new parametrization were presented in an earlier publication,[33] but in this paper, we present considerably more information about the statistical properties of the derived oscillator Hamiltonian, such as its Gaussian nature and the difference with models based on NMA-d and NMA-h_7. In addition, we present new results for model α-helices, relating to the energy gap between the amide I and amide II modes in this extended system, the delocalization length of the collective oscillations, and their coherence time.

This paper is organized as follows. In section II, we introduce the model used for the amide I and II vibrations in the protein and the description of the environmental modes. The two crucial ingredients of the model, the couplings between high-frequency modes and the properties of the interaction with the environment, are deduced from model calculations on small peptide fragments presented in Subsections II B and II C. In section III, we present the results for NMA-d_7, the dipeptide, and vibrational dynamics in a model α-helix. Section IV sums up the conclusions of this work and discusses future extensions.

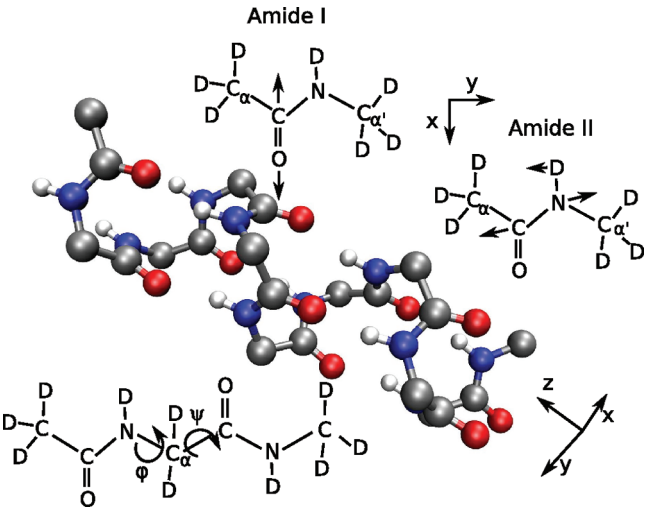

Figure 1. Cartoon of the backbone of an α-helical peptide. Each amide group contains one amide I and one amide II oscillator. A model molecule for the single amide group is NMA-d_7, which is shown in the top right corner of the figure, together with the atom movement in the amide I and II modes. In the lower left of the figure, the dipeptide used in the coupling calculation is shown.

2. MODEL

A model of vibrational dynamics should, in principle, include all modes in the peptide and solvent quantum mechanically. To simplify the calculation, we designate certain high-frequency vibrations (here, the amide I and amide II modes) as the system, which is described using quantum theory. All other modes form the environment, which influences the dynamics of vibrational energy packets in the system modes. The time evolution of the environmental modes is approximated using classical mechanics. This is a reasonable approximation because the modes that influence relaxation between the amide vibrations most are those with frequencies smaller than the joint amide I and II bandwidth. Therefore, the important bath modes have frequencies smaller than the thermal energy and can hence be described classically.

A. Fluctuating Peptide Hamiltonian. A polypeptide can be described as a chain of amide groups (see Figure 1), which we label by indices n and m. The high-frequency vibrations in each group, with excitation energies much larger than the thermal energy, are described in a quantum mechanical Hamiltonian. Indices i and j are used to distinguish between the different types of vibrations. In our case, only the amide I and amide II modes in each amide group are taken into account, which are indicated by $i = 1$ and 2, respectively. A fluctuating oscillator Hamiltonian, which includes the bilinear interactions between the high-frequency vibrations as well as their interaction with the environment, is then given by

$$H(t) = \sum_{n,i} \omega_{n,i}(t) b^{\dagger}_{n,i} b_{n,i} + \sum_{n,i;m,j} J_{n,i;m,j}(t) b^{\dagger}_{n,i} b_{m,j} - \sum_{n,i} \frac{A_i}{2} b^{\dagger}_{n,i} b^{\dagger}_{n,i} b_{n,i} b_{n,i} \quad (1)$$

dx.doi.org/10.1021/jp109431a |J. Phys. Chem. B 2011, 115, 5392–5401

The operators $b^{\dagger}_{n,i}$ and $b_{n,i}$ are the standard bosonic creation and annihilation operators on the ith mode in amide group n. The frequency and quartic anharmonicity of each mode are given by $\omega_{n,i}$ and A_i, respectively. Bilinear interactions between mode i in amide group n and mode j in group m are included as the coupling terms $J_{n,i;m,j}$.

The effect of the environment on the high-frequency modes in the system Hamiltonian is included in the time dependence of their frequencies and interactions. In effect, we will account for the environment by treating the matrix elements of the Hamiltonian as stochastic variables, whose statistics are imposed by the interaction with the fluctuating environment. We will account for fluctuations in the oscillator frequencies of the amide I and II modes and the interaction between these modes on the same amide unit. The bilinear couplings between different groups are assumed to be constant because, typically, their fluctuations are found to be much smaller than those in the oscillator frequencies. This was confirmed previously in MD simulations of trialanine, where coupling fluctuations of a few wavenumbers were found,[34] and we expect these fluctuations to be even smaller in the more rigid helix. Furthermore, as implied in the Hamiltonian, we have neglected fluctuations in the anharmonicity. The effect of such fluctuations on the spectra of the amide I mode is known to be small.[14] Finally, while correlations between the fluctuating quantities within an amide group are accounted for, we do not include correlations between different groups. This approach will allow us to parametrize the time dependence of the Hamiltonian from the simulations of a single peptide group.

We note that the fluctuating oscillator Hamiltonian has been modeled by quite a few authors for the case of amide I vibrations,[10−15] while its analogue, which also includes the amide II vibrations, has received relatively little attention.[12,29,30]

B. Fluctuations of Frequencies and On-Site Interactions. To model the statistical properties of the fluctuations in the local amide I and II vibrations and the environment-induced interactions between these vibrations within the same group, we take two steps. In the first step, we perform density functional theory (DFT) calculations on NMA-d_7 in a variety of environments of point charges and obtain a map that describes how the frequencies and the interaction depend on the electric field and its gradient at the positions of the atoms in the amide group. This is similar to the strategy followed for NMA-d in ref 29. In the second step, we use this map to obtain a fluctuating Hamiltonian from the MD trajectory of the NMA-d_7 molecule in D_2O. The trajectory, which was described earlier in ref 29, was generated at a temperature of 300 K using the GROMACS package.[35,36] DFT calculations are performed with the ADF program,[37,38] using the ADF TZ2P basis set and the RPBE exchange correlation functional.[39,40] From the DFT results, we observe that a reduced basis set of local modes accounts for most of the amide modes. This basis, which we use in the construction of the coupling map described in the next section, consists of the CC_α, $NC_{\alpha'}$, CN, and CO stretches and the OCN, DNC, NCC_α, and $CNC_{\alpha'}$ bends (see Figure 1). In the amide I vibration, 94% of the amplitude of the wave function squared is found on these modes; in the amide II vibration, this is 96%.

In NMA in heavy water, the solvent in which 2DIR experiments of polypeptides are commonly performed, the hydrogen atom bonded to nitrogen is replaced with deuterium, leading to NMA-d. Our choice to base our modeling on the fully deuterated form NMA-d_7 has been argued already in the Introduction. We have found that, in contrast to the results in NMA-d,[7,29] the heavier methyl groups in NMA-d_7 hardly move, which is essential in order to be able to use this molecule as a building block for a model of larger peptides, where the methyl groups are absent and the N atom is deuterated when performing 2DIR experiments in heavy water.

These calculations on the NMA-d_7 molecule provide a parametrization of the fluctuations in a single amide group. They define the stochastic process that governs the interaction of an amide group with the environment. The properties of this process can be arbitrary, but in the current system of amide I and II vibrations in a peptide in water, some simplifying assumptions can be made. First of all, we observe in our simulations that the fluctuations are, to a very good approximation, of Gaussian nature. In this case, all information about the fluctuations is contained in the two-point correlation functions of the fluctuating quantities.

C. Intersite Interactions. The bilinear coupling terms J in the peptide Hamiltonian (eq 1) were modeled by (electrodynamic) transition charge coupling.[18,19] For interactions between amide groups that are linked by covalent bonds, the TCC model is not applicable because mechanical coupling caused by movements of the in-between atoms (through-bond coupling) is important. Such through-bond couplings have been taken into account in models of amide I vibrations in peptides by performing DFT calculations on dipeptides or polypeptides.[10,13,18,19,34,41] Here, we extend these methods to include the amide II mode.

In order to obtain the nearest-neighbor interactions, we perform a Hamiltonian matrix reconstruction, which is based on writing the eigenmodes in a dipeptide obtained from DFT calculations as a linear superposition of the eigenmodes in two NMA-d_7 molecules. If the dipeptide eigenmodes are denoted as $|\Psi\rangle$ and the NMA-d_7 eigenmodes as $|\Phi\rangle$, the required transformation can be expressed as a 4×4 matrix T which satisfies $|\Psi\rangle = T|\Phi\rangle$. This is achieved by expressing the dipeptide eigenstates and the NMA-d_7 eigenstates in the same basis set of stretch and bend vibrations and then using a matrix reconstruction method to find the transformation between the two sets of eigenmodes.

Maps for amide I and amide II site frequencies, and the couplings, as a function of the dihedral angles (ϕ and ψ; see Figure 1) were calculated in this way. The local basis used in the NMA-d_7 molecule was introduced in section II B. Here, we denote the set of the basis states on the two sides of the dipeptide as $\{|n\rangle\}$. There are a total of 16 basis states, resulting from the 4 stretching and 4 bending basis vibrations considered on each side of the dipeptide (section II B). The expansions of the dipeptide eigenmodes, $|\Psi\rangle = \sum_n \langle n|\Psi\rangle|n\rangle$, and of the NMA-$d_7$ eigenmodes, $|\Phi\rangle = \sum_n \langle n|\Phi\rangle|n\rangle$, are known. The transformation matrix T is found by solving the system $\langle n|\Psi\rangle = \sum_m T_{nm}\langle m|\Phi\rangle$.

Because the system is overdetermined (64 equations for 16 unknowns), the transformation from the basis of dimer eigenstates to the direct product basis of NMA eigenstates is then found by a least-squares solution. Finally, the Hamiltonian in the required basis (H) is obtained by transforming the (diagonal) Hamiltonian in the basis of dipeptide eigenstates ($E_{\mathrm{dipeptide}}$) as $H = T^{+}E_{\mathrm{dipeptide}}T$. The least-squares procedure gives a transformation matrix that is not unitary, which results in a Hamiltonian in the basis of NMA states which is not exactly symmetric. We therefore explicitly symmetrize the Hamiltonian; we come back to this issue in section III B.

D. Vibrational Dynamics and Spectra. To calculate vibrational dynamics and (nonlinear) infrared spectra, we numerically integrate the time-dependent Schrödinger equation. Trajectories for the frequencies and intramode coupling in each amide group

Table 1. Electrostatic Map for the NMA-d_7 Frequencies and Coupling[a]

	ϵ_I	ϵ_{II}	J_{12}
Ω_0	1628.78	1429.17	−5.04
c_{C_x}	793.27	−966.91	−212.88
c_{C_y}	209.43	−842.78	695.18
$c_{C_{zz}}$	558.13	282.44	33.35
$c_{C_{xy}}$	−2916.53	−1627.13	−4103.32
c_{O_x}	901.51	−1000.18	−691.65
c_{O_y}	1046.21	1198.86	1284.30
$c_{O_{zz}}$	615.69	−351.50	−156.56
$c_{O_{xy}}$	−1185.40	−944.75	−1317.24
c_{N_x}	605.52	−121.05	−421.14
c_{N_y}	3039.06	196.33	1304.86
$c_{N_{zz}}$	−558.54	646.12	−376.66
$c_{N_{xy}}$	−6195.92	2069.10	407.07
c_{D_x}	−372.10	−538.13	24.39
c_{D_y}	−4313.38	1483.40	−370.65
$c_{D_{zz}}$	363.93	140.17	92.26
$c_{D_{xy}}$	−3584.54	1177.69	−857.48

[a] The map relates the amide I and II frequencies and the coupling between them to the electric field and its gradient on the atoms in the amide group. Each of these quantities, generally denoted Ω, is given by $\Omega = \Omega_0 + \sum_{a,\alpha} c_{a\alpha} E^a_\alpha$, where E^a_α is the αth Cartesian component of the field or field gradient on atom a, and the quantities c are fit parameters determined by comparing DFT results in a variety of electrostatic environments to the result of this map. The values for Ω_0 are in cm^{-1}. Units for the field and gradient coefficients are $cm^{-1}/(E_h/e\ Bohr)$ and $cm^{-1}/(E_h/e\ Bohr^2)$, respectively, where E_h is the Hartree.

Table 2. Electrostatic Map for the NMA-d_7 Dipoles[a]

	μ^x_I	μ^y_I	μ^x_{II}	μ^y_{II}
Ω_0	−0.243	0.070	−0.021	0.283
c_{C_x}	−0.701	−2.174	−2.735	1.891
c_{C_y}	1.216	−4.310	−4.683	−1.201
$c_{C_{zz}}$	0.393	−1.139	0.025	−0.586
$c_{C_{xy}}$	5.064	−18.600	−18.087	−1.570
c_{O_x}	1.532	−2.059	−1.308	0.229
c_{O_y}	−1.498	8.961	8.854	0.122
$c_{O_{zz}}$	0.555	−0.296	0.332	−0.200
$c_{O_{xy}}$	0.593	−7.058	−7.891	0.766
c_{N_x}	0.394	0.778	0.966	−0.537
c_{N_y}	1.561	2.747	3.911	−8.661
$c_{N_{zz}}$	0.559	−0.238	−0.243	−0.898
$c_{N_{xy}}$	−1.595	−0.924	0.184	4.448
c_{D_x}	−0.477	−0.728	−0.937	1.211
c_{D_y}	−1.005	−0.677	−0.815	5.138
$c_{D_{zz}}$	1.208	0.550	1.580	−2.126
$c_{D_{xy}}$	−0.310	−1.599	−0.964	3.780

[a] The values for Ω_0 are in Debye. Units for the field and gradient coefficients are Debye/(E_h/e Bohr) and Debye/(E_h/e Bohr^2), respectively, where E_h is the Hartree. The notation is similar to that in Table 1; the field dependent quantities are now the components of the transition dipole.

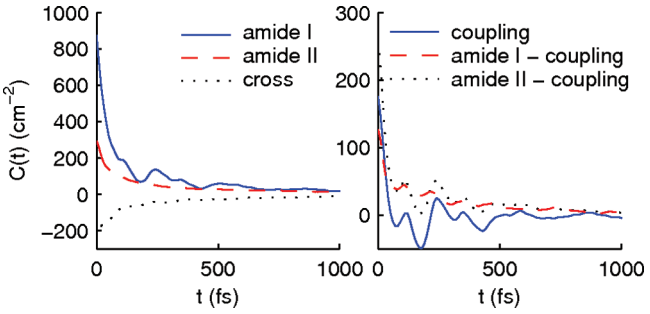

Figure 2. Correlation functions in NMA-d_7 found from our DFT maps in combination with MD trajectories. To the left are shown the autocorrelation functions for the amide I and amide II frequencies and their cross-correlation, while to the right, the autocorrelation is shown for the coupling between both vibrational modes and the cross-correlation between the coupling and both vibrational frequencies.

were generated from the auto- and cross-correlation functions calculated and presented in section III A. This procedure assumes that the fluctuations are Gaussian (see below).

Two-dimensional infrared spectra were calculated by propagating the time-dependent Schrödinger equation during the coherence times t_1 and t_3 and the population time t_2 for the various orientational contributions to the signal.[42,43] The most time-consuming part in the calculation is the propagation of coherent superpositions of one- and two-exciton states during t_3. This propagation is simplified significantly by using the Trotter formula to factorize the propagation in each time step into a part due to the harmonic terms in the Hamiltonian and a part arising from the anharmonicities. The time propagation from the anharmonic part is trivial, and the harmonic two-quantum propagator can be written as the product of one-quantum propagators using a version of Wick's theorem.[44]

3. RESULTS AND DISCUSSION

A. NMA-d_7. The obtained DFT maps which describe the response to an electrostatic environment of the frequencies of the amide I and II oscillators and their coupling within the same amide unit are given in Table 1, while the response of the transition dipoles of both vibrations to such an environment is given in Table 2. These maps were used to obtain a fluctuating Hamiltonian from the MD trajectory of the NMA-d_7 molecule in D_2O. We characterize the trajectories for the Hamiltonian matrix elements by plotting their (two-point) auto- and cross-correlation functions in Figure 2. They show many features similar to the correlation functions of NMA-d, such as the clear anticorrelation between the frequencies and the large fluctuations in the coupling. Two differences are the smaller fluctuation amplitude of the amide I mode and the presence of correlation between the coupling and the amide I frequency in the NMA-d_7 molecule. We have confirmed that the fluctuations are indeed, to a large extent, Gaussian by studying various multipoint correlation functions, two of which are shown in Figure 3.

It turns out that the DFT calculation overestimates the energy gap between the two modes, which results in a calculated linear spectrum with the amide I and amide II peaks too far apart. This is not entirely surprising because it is well-known that DFT frequencies are only accurate within a few percent. They are often scaled to correct for rather systematic errors.[45] We therefore multiply the energies obtained in the DFT calculation by a scaling factor, which is c_1 for the amide I mode and c_2 for the amide II mode. Because, as far as we know, no gas-phase spectra

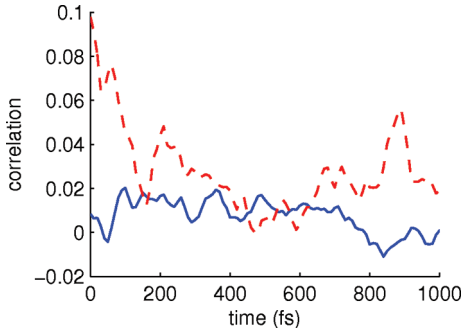

Figure 3. Lowest-order non-Gaussian contributions to the fluctuations in the amide I frequency in NMA-d_7. The solid line shows a three-point correlation function $\langle\omega^2(t)\omega(0)\rangle/\sigma^3$, the dashed line the non-Gaussian contribution to a four-point correlation function, $(\langle\omega^2(t)\omega^2(0)\rangle - 2\langle\omega(t)\omega(0)\rangle^2 - \sigma^4)/\sigma^4$. The correlation functions are normalized by powers of $\sigma^2 = \langle\omega^2(t)\rangle$. Non-Gaussian contributions to the fluctuations in the amide II frequency and the coupling are smaller than 1%.

of NMA-d_7 have been measured, it is not possible to use gas-phase experimental results to find the scaling factors. It is, however, possible to compare the average energy gap in the liquid to the experimental spectrum. Following this procedure, we obtain scaling factors of $c_2 = 1.0248$ for the amide II mode and $c_1 = 0.9693$ for the amide I mode. In this way, we correct for possible differences between the DFT energies and the unknown experimental gas-phase frequencies, as well as for possible errors in the predicted solvent shift. Thus, we are not able to asses the reliability of the prediction of the solvent shift, which turned out to be predicted rather poorly in NMA-d.[29] After the scaling using the gas-phase eigenmodes as a basis, the average values of the diagonal elements of the Hamiltonian in solution obtained from the MD simulations are 1514 and 1586 cm^{-1}, respectively. On this basis, the Hamiltonian is not diagonal, and the average coupling between the two modes is 36.7 cm^{-1}, induced by the solvent. The average of the eigenfrequencies, which are calculated from each MD snapshot, are found to be 1495 and 1605 cm^{-1} for amide II and amide I, respectively. This is in good agreement with the experimentally obtained peak positions (1495 and 1604 cm^{-1}; ref 5). The DFT simulation also yields the parameters needed in the TCC coupling model; for completeness, they are collected in Table 3.

Other parameters that we use in the peptide model are the anharmonicities, the dipole vectors, and the time correlation functions of the amide I and II modes. The anharmonicities are taken to be 16 cm^{-1} for the amide I mode[1] and 11 cm^{-1} for the amide II mode.[5] From the average over the MD trajectory, the angle between the two dipoles is 79.4° (which compares well to the 75° found experimentally in ref 5), and the length of the amide II dipole is 0.64 times the length of the amide I dipole.

In the 2D experiment, broad-band laser pulses are used to excite the amide I and II bands coherently. Interaction with the laser light prepares a coherent superposition of the Hamiltonian eigenstates at a point in time. During the evolution time following the pulse, the dynamic environment changes the character of instantaneous system eigenstates. In principle, matrix elements of the propagator between all eigenstates at different points in time exist. The dynamics then leads to redistribution of energy over the instantaneous eigenstates, which also implies relaxation of energy toward the equilibrium configuration. The two-dimensional spectrum can be interpreted as the presence of excitations at a certain

Table 3. Parameters of the TCC Model for the Amide I and Amide II Modes As Obtained from Quantum Chemical Calculations on a NMA-d_7 Molecule[a]

	C_α	C	O	N	D	$C_{\alpha'}$
q	0.11337	0.36621	−0.53731	−0.48052	0.24280	0.29545
dq_1	0.01689	−0.02838	−0.01569	0.01729	0.00002	0.00986
v_{1x}	0.00705	0.02179	−0.00695	−0.02782	−0.12236	−0.00542
v_{1y}	−0.05670	0.82436	−0.50410	−0.07861	−0.08970	0.00772
dq_2	−0.01558	0.00778	−0.00734	0.00686	0.01117	−0.00289
v_{2x}	−0.11582	0.57803	−0.05830	−0.53197	0.51119	0.11755
v_{2y}	0.03083	0.01505	0.05996	−0.0065	−0.04563	−0.02573

[a] The charges q and charge derivatives dq on the methyl groups have been summed into the values listed as C_α. The displacements v are given as a fraction of the oscillator amplitude, which is 0.028811 Å for the amide I mode and 0.037201 Å for the amide II mode. Charges are in units of e. The coordinate system is defined as that in Figure 1.

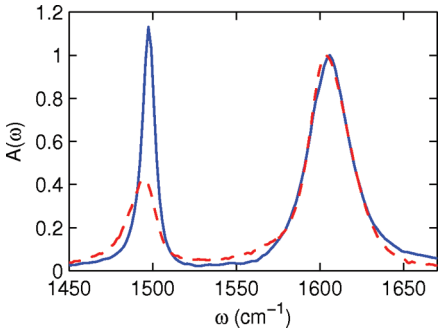

Figure 4. Calculated (solid line) linear absorption spectrum of NMA-d_7 in heavy water compared with experimental results (dashed line) from ref 5.

energy ω_1 before the waiting time (plotted on the horizontal axis), correlated with the presence of an energy packet at ω_3 after the waiting time (plotted on the vertical axis). In this interpretation, the various points in the 2DIR spectrum follow the relaxation process between sets of instantaneous eigenmodes with the same energy. One must note, however, that this simplified interpretation neglects the coherent superpositions of two eigenmodes that can also be prepared by the first two pulses.

The calculated linear and 2DIR spectra, obtained by propagating the Schrödinger equation with the time-dependent Hamiltonian given in eq 1,[43] are shown in Figures 4 and 5, respectively, together with the experimental spectra from ref 5. The line shape of the amide I mode is predicted well by the calculations. In the amide II region, the agreement is not as good. The amide II peak is too narrow, indicating that the calculation underestimates the time scale or the amplitude of the fluctuations. The calculation also overestimates the dipole of the amide II vibration; the ratio between the integrated intensities of the two modes is 0.4 in the calculation versus 0.3 in the experiment. The relative intensity of the cross peak in the parallel and the perpendicular polarization geometry is well-reproduced in the simulations, reflecting the correct prediction of the relative angle between the amide I and amide II transition dipoles.

B. Dipeptide. The Hamiltonian matrix reconstruction for a dipeptide explained in section II C gives values for the amide I and II frequencies at the C and the N side of the dipeptide, the intrasite coupling at both sides, and the four intersite couplings. The maps of these values obtained as a function of the dihedral angles are given in Figures 6 and 7.

dx.doi.org/10.1021/jp109431a |J. Phys. Chem. B 2011, 115, 5392–5401

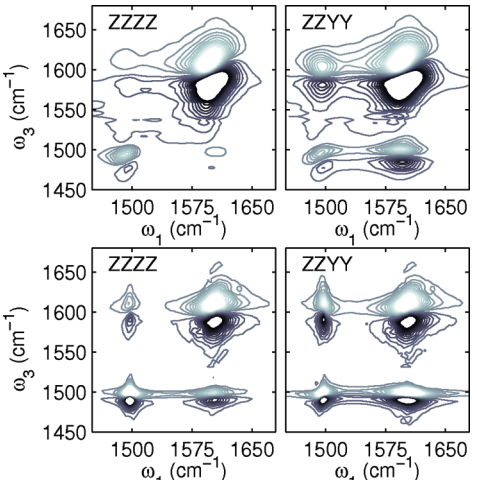

Figure 5. Experimental (top row, ref 5) and simulated (bottom row) 2DIR spectra of NMA-d_7 in heavy water for the *ZZZZ* (parallel) and *ZZYY* (perpendicular) polarization geometries. Twenty-five equally spaced contours are plotted between −60 and 60% of the maximum amplitude in each spectrum. Gray contours are used for bleaching/stimulated emission peaks, while induced absorption peaks are plotted in black.

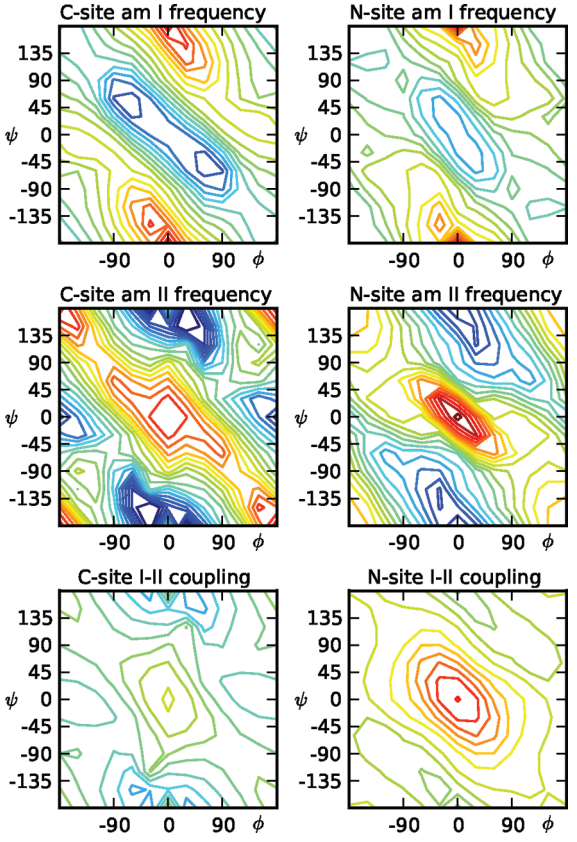

Figure 6. Amide I and amide II frequencies and amide I−amide II on-site coupling constants as a function of Ramachandran angles ϕ and ψ (in degrees). Contours for negative (blue) and positive (red, yellow) values are plotted every 5 cm^{-1} from −50 to 50 cm^{-1}. In the frequency panels, the average frequencies are subtracted.

Before discussing our results, we come back to the fact that our construction gives a basis transformation connecting the dipeptide eigenstates to the direct product of eigenstates of two NMA

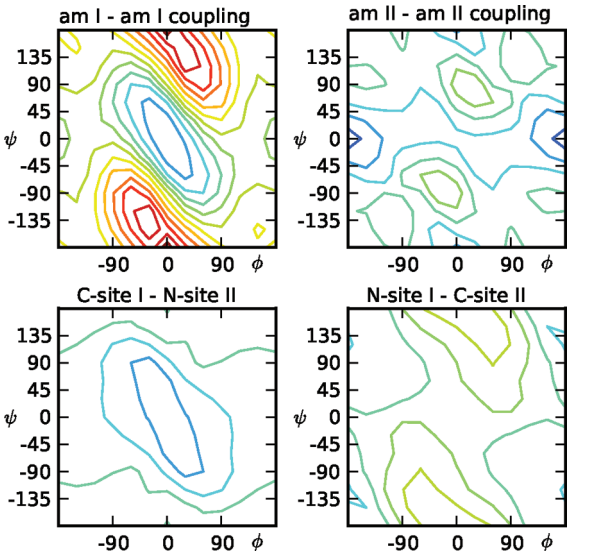

Figure 7. Ramachandran map for the couplings between the two sites of the dipeptide, obtained from matrix reconstruction using DFT calculations as the starting point. The dihedral angles ϕ and ψ are given in degrees. Contours for negative (blue) and positive (red, yellow) values are plotted every 2.5 cm^{-1} from −17.5 to 17.5 cm^{-1}.

molecules that is only approximately unitary (section II C). As a result, the Hamiltonian in the NMA basis is not completely symmetric. We corrected for this unphysical result by explicitly symmetrizing the Hamiltonian. This leads only to small corrections of the couplings, as we have checked by comparing with a (nonlinear) minimization procedure that explicitly constrains the transformation matrix to be unitary. In that procedure, we minimize the difference between the known dipeptide normal modes and the transformation matrix times the NMA normal modes. Minimization is done with respect to the Frobenius norm (least-squares) and is constrained to a unitary transformation matrix. The matrix elements reconstructed in this way differ from the ones obtained after symmetrization by less than 0.32 cm^{-1}.

Several previous maps have been presented for the amide I frequency and intersite coupling in a dipeptide. Couplings were calculated as the finite difference of the energy along a vibrational coordinate[18,41] or by matrix reconstruction methods.[10,13,19,34] Our results, which are found using joint inversion of the amide I and amide II modes, give qualitatively the same results as those works for the amide I−amide I intersite coupling. All maps find a negative coupling along the antidiagonal ($\psi = -\phi$) and positive couplings in the remaining corners. However, quantitative differences between the maps are significant. In the Torii and Tasumi map, the coupling varies between −9.5 and 32.7 cm^{-1}.[41] This asymmetry between positive and negative values of the coupling is also found in our present result, while the extremal values are almost equal in refs 19 and 31. Furthermore, although reconstruction of the couplings between amide I units seems to be rather robust, values for the frequency shifts strongly depend on the DFT method used, as concluded in ref 34. We leave a detailed comparison of DFT methods in the joint amide I−amide II case for future work. In the present work, we will apply the maps to a system where all sites experience the same shift and the absolute value will only affect the distance between the amide I and the amide II bands.

Calculations on the amide I, II, III, and A modes in a dipeptide with hydrogen instead of deuterium atoms have also been

reported.[31] The difference between deuterium and hydrogen in the methyl groups is apparent in the vibrational frequencies in NMA-h_7 and NMA-d_7 found using DFT; in NMA-d_7, we obtain 1373 and 1666 cm^{-1} for the amide II and amide I modes, respectively, while Hayashi and Mukamel report 1472 (1507) and 1722 cm^{-1} (1733 cm^{-1}) for frozen (flexible) methyl groups.[31] However, many of the qualitative features of the frequency and coupling maps, as extracted from the dipeptide and NMA calculations, agree. The coupling strengths between amide I modes for both dihedral angles close to 0 are significantly more negative in the nondeuterated map. In the amide II−amide II coupling map, we observe positive regions around $(\phi,\psi) = (30°,80°)$ that are not so clear in the Hayashi−Mukamel map. Only one of the two amide I−amide II maps is given in ref 31. The map presented here for the coupling between the N-site amide I mode and the C-site amide II mode is distinctly different from the coupling map between the N-site amide II mode and the C-site amide I mode. This is not surprising because the distance and bonding patterns are entirely different for the two cases. Recently, Ge and co-workers have calculated amide I−amide II coupling maps by taking numerical derivatives of the energy along the normal-mode coordinates.[28] With our method of matrix reconstruction, we find similar results.

C. α-Helix: Hamiltonian. As a model polypeptide, we consider an α-helix. To construct the helix, we use standard bond lengths and angles[46] and take all pairs of dihedral angles to be $(\phi,\psi) = (-57°,-47°)$.

The fluctuations in the amide I and II site energies and in the coupling between them are parametrized from our NMA-d_7 results. With the assumption that the fluctuations are Gaussian, all information is contained in the six auto- and cross-correlation functions $C(t)$, shown in Figure 2. Cross-correlations between the two frequencies on the same group and the intragroup coupling are included, but as noted in section II A, we assume that the fluctuations in different groups are uncorrelated. Such correlations might be present, especially between the amide II and amide I vibrations in amide groups connected through a hydrogen bond. Detailed tests would require the combination of our map with MD simulations of peptide fragments, which is beyond the scope of this paper. Assuming no intergroup correlations, a fluctuating Hamiltonian for a helix with N amide groups can be generated from the NMA-d_7 correlation functions.

In this model, we make the usual assumption that the intergroup couplings are constant in time. This can be rationalized from the origin of these couplings as electrodynamic or through-bond interactions, which are not expected to exhibit large fluctuations.[47,48] Coupling constants in the helix, obtained from the transition charge coupling model combined with the dipeptide DFT map, are given in Table 4. In the helix, large couplings are found between the amide I modes that are connected along the backbone and through intramolecular hydrogen bonds. These interactions are quantitatively similar, in agreement with earlier work.[47,49] The couplings in the amide I band that we find are also in reasonable agreement with experimental results, which read $J^{I}_{12} = 8.5 \pm 1.8$ cm^{-1}, $J^{I}_{13} = -5.4 \pm 1.0$ cm^{-1}, and $J^{I}_{14} = -6.6 \pm 0.8$ cm^{-1}.[50] While the couplings in the amide I band are rather well-known, much less information is available for the amide II modes. One model empirically included an amide II−amide II nearest-neighbor coupling of −8.7 cm^{-1}.[51] This is considerably larger than the coupling constants found in our calculation (Table 4). The discrepancy can be understood from the fact that the empirical model used in ref 51 includes only interactions between nearest-neighbor amide II oscillators. Perhaps surprisingly, in our results, the largest interaction between amide II modes skips one peptide unit along the backbone. This large coupling can be rationalized by observing that the CN bonds in these units make an angle of only 13°. Because the stretch vibrations of these bonds form the major contribution to the amide II mode, this geometry will increase the coupling. Further calculations on the couplings between amide II modes were performed in ref 31. The trend of the couplings agrees with our results, $J^{II}_{n,n+1}$ and $J^{II}_{n,n+3}$ are small, the largest coupling is $J^{II}_{n,n+2}$, which is negative, and $J^{II}_{n,n+4}$ is positive.

Table 4. Intersite Coupling Constants in a Model α-Helix in cm^{-1}, Obtained from a Combination of the TCC Model with the Nearest-Neighbour Coupling Map[a]

	$n+1$	$n+2$	$n+3$	$n+4$	$n+5$	$n+6$
am I−am I	6.0	−3.7	−6.8	−2.3	−0.8	−0.6
am II−am II	−1.3	−4.7	−0.1	1.4	−0.6	−0.3
am II−am I	−4.6	−1.2	−1.1	0.2	0.0	−0.2
am I−am II	1.6	−8.8	−9.5	3.3	−0.7	−0.9

[a] The amide groups are indexed from the N terminal to the C terminal.

Table 5. Shifts in the Frequencies and in the on-Site Coupling on the N and C Sites of a Dimer Obtained from the DFT Map for the α-Helix Configuration, in cm^{-1}

	N site	C site	sum
amide I frequency	16.9	12.7	29.6
amide II frequency	−9.2	−26.4	−35.6
on-site coupling	13.9	−6.2	7.7

Apart from the first and the last groups, each amide group in the helix has two neighbors. The presence of these neighbors shifts the frequencies and the intragroup coupling. From the dipeptide DFT map, these shifts can be determined, and their values in the α-helix geometry are given in Table 5. For a group in the middle of a helix, the shifts from right and left neighbors must be added.[15,19] We assume that the average frequency in each group is the same, which is only correct for groups in the middle of a long helix.[47,52,53]

D. α-Helix: Vibrational Dynamics and Spectra. In the peptide Hamiltonian, we have included the frequency shifts found from the dipeptide map, shown in Figure 6. Because of the combination of a blue-shifted amide I frequency, a red-shifted amide II frequency, and an increased coupling, the gap between the two bands is larger than that in NMA-d_7. This is in agreement with experimental results on α-helix forming polylysine.[51] In our calculations, the increase in the frequency gap leads to slower relaxation between the amide I and II modes. While a relaxation constant of 0.5−0.7 ps was found in NMA-d,[7,29] the current parametrization yields a value of 2 ps for the helix.[33] Such a shift in the vibrational frequencies, caused by interactions with neighboring peptide groups, could explain the experimentally observed difference in lifetime of the amide I mode between NMA and larger peptides.[1]

Figure 8 shows the density of states and the participation number spectrum for snapshots of the Hamiltonian at a fixed point in time. The latter quantity provides a measure of the delocalization of the collective vibrational states in a dynamic environment.[47] It is

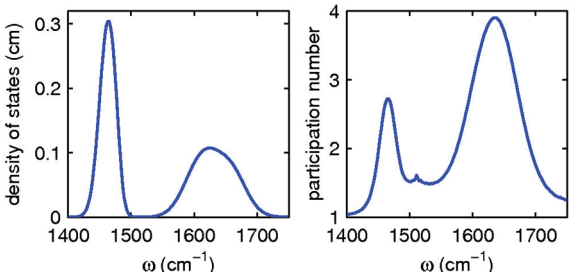

Figure 8. Density of instantaneous normal modes (left panel) and participation number spectrum (right panel) for a helix with 10 amide units.

defined by considering the eigenstates of the Hamiltonian $\Psi_u(t)$ at each point in time and calculating the participation number as

$$R(\omega) = \langle \sum_u (\sum_n \Psi_{un}^4(t))^{-1} \delta(\omega - E_u) \rangle / \langle \sum_u \delta(\omega - E_u(t)) \rangle \quad (2)$$

where $E_u(t)$ is the energy of eigenstate Ψ_u at time t. The average is over all snapshots. From the calculated density of states, we observe that there is a small gap between the amide I and II modes. This means that it is possible to distinguish between the two modes, even though they are coupled. The density of states in the amide II band is much larger than that in the amide I band, which should be expected as a result of the difference in intersite coupling strengths in the two bands. The participation number spectrum shows that amide I vibrations are delocalized over almost four amide groups, while the amide II vibrations are somewhat more localized. The value in the amide I band agrees reasonably well with the results of Ham et al.[47] Similar localization sizes in the amide I band have also been found in experimental work on 3_{10} helices.[25] The delocalization pattern for both types of helices might be different, however.

Figure 9 shows 2DIR spectra for the α-helix calculated for several waiting times and polarization geometries. The peaks in this spectrum are further apart than those in the spectrum of NMA-d_7 in Figure 5. This is mostly a result of the shifts in the amide I and II frequencies and their coupling due to neigboring peptide groups, as mentioned in the beginning of this section. Compared to NMA spectra, more structure is observed in the amide I peak resulting from the A and E_1 type eigenstates also observed experimentally.[54] The splitting in the simulated spectrum is slightly exaggerated compared to the experimental observation. Like in the NMA-d_7 spectrum, cross peaks between amide I and II modes are clearly observed, showing that these two modes are still strongly coupled in the helix. The amide I−amide II cross peaks are stronger in the perpendicular polarization configuration, as expected from their almost perpendicular transition dipole vectors. The intensity of the cross peaks changes in a complex way with the waiting time t_2, reflecting partially coherent exciton transport between the two bands. This was discussed in more detail in our previous paper.[33] There, we further demonstrated that it is possible to disentangle the intra- and interband dynamics by analyzing the relative peak intensities.

Insight into the vibrational dynamics during the waiting time can also be gained from the perspective of local modes. Starting from a picture of amide I and II vibrations in the various amide groups, vibrational dynamics corresponds to the movement of energy packets through space. Because the wavelength of the light is much larger than the size of a peptide, the laser excites all vibrations coherently. Because of symmetry, movement to the right or to the left along the helix is equally probable, and on average, no net energy transfer will occur. Nevertheless, information on the transport of vibrational energy through space, which can be directly characterized in simulation by starting from a localized vibration, can be extracted from detailed analysis of the 2DIR spectra for different polarization geometries.[33] The presence of partially delocalized eigenstates leads to coherent, wave-like transport along the helix for short times. Because of the dynamic destruction of the instantaneous eigenstates, coherent transport is only possible for about 500 fs. Afterward, the transport in the site basis can be characterized as diffusive.

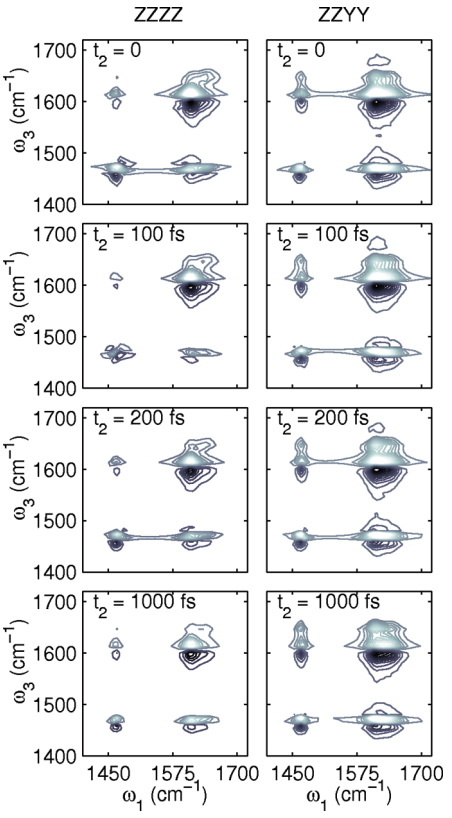

Figure 9. Calculated 2DIR spectra for the model α-helix as a function of waiting time for parallel and perpendicular polarization geometries. Contours are plotted at 25 equally spaced levels between −60 and 60% of the maximum amplitude in the $t_2 = 0$ spectra. Gray contours are used for bleaching/stimulated emission peaks, while induced absorption peaks are plotted in black.

The role of coherent transport in the helix can be further clarified by directly looking at the off-diagonal matrix elements of the density matrix in the site basis. A few of them are plotted in Figure 10. In the simulations, a single amide I local mode was excited at time $t = 0$. The lifetime of the coherence was found to be on the order of 500 fs−1 ps. Such amide I−amide II coherences have been reported experimentally in the amide II peak of NMA-d_7 in D_2O with a lifetime of 150 fs but, to our knowledge, not in experiments on larger peptides. The latter is possibly due to the limited number of data sets where the waiting time is varied.

We thus find that coherent transport is important in the amide I and II modes in an α-helix on a time scale up to a few hundred

dx.doi.org/10.1021/jp109431a |J. Phys. Chem. B 2011, 115, 5392–5401

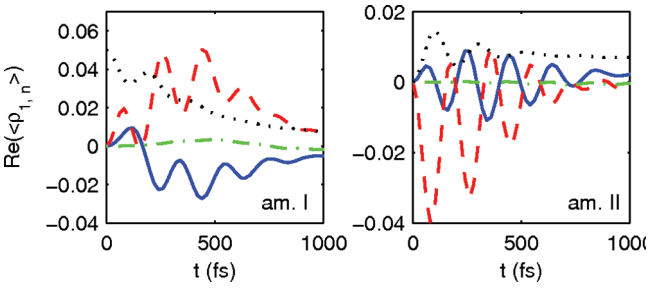

Figure 10. Coherences within the amide I (left panel) and amide II (right panel) bands on amide group n and m, for (n,m) equal to (1,2) (solid line), (1,4) (dashed line), and (7,8) (dash−dotted line). The dotted line indicates the population on group 1, scaled down by a factor of 20. Data were obtained by simulation of a model α-helix of 10 groups, which are numbered starting at the N terminus of the helix. All quantities are ensemble-averaged. At time $t = 0$, the amide I vibration on group 1 was excited.

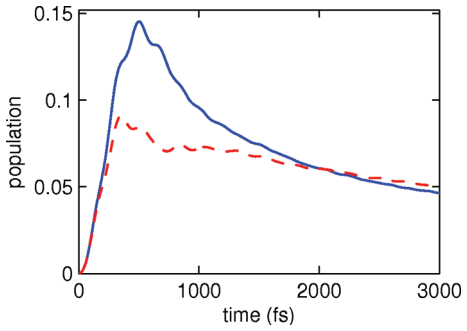

Figure 11. Amide I population on the fourth amide group of an α-helix following initial excitation of the amide I vibration on the first group. The solid line presents the data for a helix where all sites have the same average oscillator frequency, while the dashed line corresponds to a system where the amide I vibration on the first group is shifted down by 30 cm^{-1} relative to all other amide I oscillators.

femtoseconds. This calculation applies to a perfect helix, in which localization is only induced by the dynamic environment. Recent experiments have also considered a different situation, in which one of the amide oscillators has a different environment, leading to a shift in the vibrational frequency.[55] This allows the specific excitation of a local mode. If the shift is significantly larger than the coherent couplings, one would expect perfect localization and strong suppression of coherent energy transfer to the other local modes. However, the environment-induced fluctuations are large enough to make transport possible. To demonstrate this, we plot the population on the fourth amide I mode as a function of waiting time, following initial excitation of the first amide I mode (Figure 11). Comparing the situation in which the initially excited mode is shifted by −30 cm^{-1} with an unshifted initial excitation, we find that the maximum of the transferred population is roughly halved. However, significant transfer is still possible, and the time scale on which energy flows away from the shifted amide I mode is almost the same as that in the unshifted case.

4. CONCLUSIONS

In this paper, we have presented an electrostatic map for the effect of the environment on the amide I and II frequencies, as well as their coupling, in NMA-d_7. The map is more suitable for the parametrization of these modes in larger polypeptides than earlier maps based on NMA-d, which suffered from contributions of the methyl umbrellas to the amide II mode. The combination with MD simulation allows the comparison of calculated linear and nonlinear spectra with experiment. Correspondence is excellent for the amide I mode. Reasonable results are obtained for the amide II mode, although further improvement is necessary. The modeling reveals strong coupling between the amide I and II modes (on the order of 10 cm^{-1}), which is reflected in the presence of a cross peak in the 2DIR spectra, in agreement with experiment.

To be able to model larger peptides, we have calculated couplings between amide I and II modes in different amide groups from a transition charge coupling model. Because such models cannot properly reproduce the couplings between modes in neighboring amide groups, we used matrix reconstruction methods to create a joint amide I−amide II coupling map from DFT calculations on a dipeptide. Apart from the couplings, the calculations predict that the energy gap between the two modes is larger in a polypeptide than that in NMA-d_7, which leads to slower interband relaxation. These findings for the energy gap and the relaxation time agree with experimental data.

Using these parametrizations, we have studied the vibrational dynamics in a model α-helix. Coherent transport is possible within the first 0.5−1 ps after excitation. Similarly, also, vibrational coherence survives over this time scale. We find that even if the frequency of an initially excited amide mode in the α-helix is shifted by 30 cm^{-1} compared to all other oscillators, significant transport of energy over the helix is still possible within 1 ps. The precise strength of this mechanism depends strongly on the magnitude of the environment-induced fluctuations. Because our model does not include the lower exposure to the solvent in a helix as compared to NMA, it probably overestimates the size of the frequency fluctuations. The neglect of backbone fluctuations on the other hand can be expected to result in an underestimation of the frequency fluctuations. Considering previous studies, where water-exposed sites were found to have a broader frequency distribution than buried sites,[23,24,56] the former effect is likely to dominate, leading to a slight overall overestimation of the frequency fluctuations in this work. If the fluctuations in a realistic system are indeed smaller, the escape of a vibration from an oscillator with a shifted energy will be suppressed. However, smaller fluctuations will also lead to even longer lived coherences in the ideal helix. In future studies, the precise properties of the fluctuations in larger peptides should be investigated, employing MD simulations on these structures. Such simulations can also answer the interesting question of the correlation of fluctuations between different amide groups, which could further enhance the coherent transport.

In this work, we have added the amide II mode as a relaxation channel for excited amide I vibrations. The model Hamiltonian conserves the number of excitations in these two modes combined. In reality, vibrational relaxation to other modes will also occur. Inclusion of these processes is a challenging problem, which can be tackled by extending the simulations presented here using nonequilibrium MD simulations.[4,57] Such simulations should also address the back-reaction of the system to the environment to ensure correct thermalization, which can be included using mean-field theory.[58]

■ ASSOCIATED CONTENT

Supporting Information. All of the data for the maps developed in this paper are provided. This material is available free of charge via the Internet at http://pubs.acs.org.

■ AUTHOR INFORMATION

Corresponding Author

*E-mail: j.knoester@rug.nl.

Present Addresses

[†]Now at the Department of Chemistry, Graduate School of Science, Kyoto University, Kyoto 606−8502, Japan.

■ ACKNOWLEDGMENT

One of the authors (T.l.C.J) acknowledges The Netherlands Organisation for Scientific Research (NWO) for support through a VIDI grant.

■ REFERENCES

(1) Hamm, P.; Lim, M.; Hochstrasser, R. M. *J. Phys. Chem. B* **1998,** *102,* 6123.

(2) Ganim, Z.; Chung, H. S.; Smith, A. W.; DeFlores, L. P.; Jones, K. C.; Tokmakoff, A. *Acc. Chem. Res.* **2008,** *41,* 432.

(3) Fujisaki, H.; Stock, G. *J. Chem. Phys.* **2008,** *129,* 134110.

(4) Nguyen, P. H.; Park, S.-M.; Stock, G. *J. Chem. Phys.* **2010,** *132,* 025102.

(5) DeFlores, L. P.; Ganim, Z.; Ackley, S. F.; Chung, H. S.; Tokmakoff, A. *J. Phys. Chem. B* **2006,** *110,* 18973.

(6) DeFlores, L. P. *Multi-mode Two-dimensional Infrared Spectroscopy of Peptides and Proteins*. Ph.D. Thesis, Massachussetts Institute of Technology, Cambridge, MA, 2008.

(7) Dijkstra, A. G.; Jansen, T. l. C.; Bloem, R.; Knoester, J. *J. Chem. Phys.* **2007,** *127,* 194505.

(8) Zhang, Y.; Fujisaki, H.; Straub, J. E. *J. Phys. Chem. A* **2009,** *113,* 3051.

(9) Torii, H.; Tasumi, M. *J. Chem. Phys.* **1992,** *96,* 3379.

(10) Choi, J. H.; Ham, S.; Cho, M. *J. Phys. Chem. B* **2003,** *107,* 9132.

(11) Schmidt, J. R.; Corcelli, S. A.; Skinner, J. L. *J. Chem. Phys.* **2004,** *121,* 8887.

(12) Hayashi, T.; Zhuang, W.; Mukamel, S. *J. Phys. Chem. A* **2005,** *109,* 9747.

(13) Watson, T. M.; Hirst, J. D. *Mol. Phys.* **2005,** *103,* 1531.

(14) Jansen, T. l. C.; Knoester, J. *J. Chem. Phys.* **2006,** *124,* 044502.

(15) Gorbunov, R. D.; Stock, G. *Chem. Phys. Lett.* **2007,** *437,* 272.

(16) Torii, H. *Mol. Phys.* **2009,** *107,* 1855.

(17) Lin, Y.-S.; Shorb, J. M.; Mukherjee, P.; Zanni, M. T.; Skinner, J. L. *J. Phys. Chem. B* **2009,** *113,* 592.

(18) Hamm, P.; Woutersen, S. *Bull. Chem. Soc. Jpn.* **2002,** *75,* 985.

(19) Jansen, T. l. C.; Dijkstra, A. G.; Watson, T. M.; Hirst, J. D.; Knoester, J. *J. Chem. Phys.* **2006,** *125,* 044312.

(20) Jansen, T. l. C.; Knoester, J. *Biophys. J.* **2008,** *94,* 1818.

(21) Ganim, Z.; Tokmakoff, A. *Biophys. J.* **2006,** *91,* 2636.

(22) Ganim, Z.; Jones, K. C.; Tokmakoff, A. *Phys. Chem. Chem. Chem. Phys.* **2010,** *12,* 3579.

(23) Woys, A. M.; Lin, Y.-S.; Reddy, A. S.; Xiong, W.; de Pablo, J. J.; Skinner, J. L.; Zanni, M. T. *J. Am. Chem. Soc.* **2010,** *132,* 2832.

(24) Manor, J.; Mukherjee, P.; Lin, Y.-S.; Leonov, H.; Skinner, J. L.; Zanni, M. T.; Arkin, I. T. *Proc. Natl. Acad. Sc. U.S.A.* **2006,** *103,* 3528.

(25) Maekawa, H.; Formaggio, F.; Toniolo, C.; Ge, N. H. *J. Am. Chem. Soc.* **2008,** *130,* 6556.

(26) Wang, J.; Zhuang, W.; Mukamel, S.; Hochstrasser, R. M. *J. Phys. Chem. B* **2008,** *112,* 5930.

(27) Kobus, M.; Nguyen, P. H.; Stock, G. *J. Chem. Phys.* **2010,** *133,* 034512.

(28) Maekawa, H.; Poli, M. D.; Moretto, A.; Toniolo, C.; Ge, N. H. *J. Phys. Chem. B* **2009,** *113,* 11775.

(29) Bloem, R.; Dijkstra, A. G.; Jansen, T. l. C.; Knoester, J. *J. Chem. Phys.* **2008,** *129,* 055101.

(30) Maekawa, H.; Ge, N. H. *J. Phys. Chem. B* **2010,** *114,* 1434.

(31) Hayashi, T.; Mukamel, S. *J. Phys. Chem. B* **2007,** *111,* 11032.

(32) Ham, S.; Cha, S.; Choi, J.; Cho, M. *J. Chem. Phys.* **2003,** *119,* 1451.

(33) Dijkstra, A. G.; Jansen, T. l. C.; Knoester, J. *J. Phys. Chem. A* **2010,** *114,* 7315.

(34) Gorbunov, R. D.; Kosov, D. S.; Stock, G. *J. Chem. Phys.* **2005,** *122,* 224904.

(35) Berendsen, H. J. C.; van der Spoel, D.; van Drunen, R. *Phys. Commun* **1995,** *91,* 43.

(36) Lindahl, E.; Hess, B.; van der Spoel, D. *J. Mol. Model.* **2001,** *7,* 306.

(37) te Velde, G.; Bickelhaupt, F. M.; Baerends, E. J.; Fonseca Guerra, C.; van Gisbergen, S. J. A.; Snijders, J. G.; Ziegler, T. *J. Comput. Chem.* **2001,** *22,* 931.

(38) Guerra, C. F.; Visser, O.; Snijders, J. G.; te Velde, G.; Baerends, E. J. *Methods and techniques in computational chemistry, metecc-S*; STEF: Cagliari, 1995.

(39) Perdew, J. P.; Burke, K.; Ernzerhof, M. *Phys. Rev. Lett.* **1996,** *77,* 3865.

(40) Hammer, B.; Hansen, L. B.; Norskov, J. K. *Phys. Rev. B* **1999,** *59,* 7413.

(41) Torii, H.; Tasumi, M. *J. Raman Spectrosc.* **1998,** *29,* 81.

(42) Torii, H. *J. Phys. Chem. A* **2006,** *110,* 4822.

(43) Jansen, T. l. C.; Knoester, J. *J. Phys. Chem. B* **2006,** *110,* 22910.

(44) Paarmann, A.; Hayashi, T.; Mukamel, S.; Miller, R. J. D. *J. Chem. Phys.* **2009,** *130,* 204110.

(45) Jensen, F. *Introduction to Computational Chemistry*; Wiley: Chicester, U.K., 1999.

(46) Lehninger, A. L. *Biochemistry*; Worth Publishers: New York, 1975.

(47) Ham, S.; Hahn, S.; Lee, C.; Kim, T.; Kwak, K.; Cho, M. *J. Phys. Chem. B* **2004,** *108,* 9333.

(48) Kobus, M.; Gorbunov, R. D.; Nguyen, P. H.; Stock, G. *Chem. Phys.* **2008,** *347,* 208.

(49) Choi, J.; Hahn, S.; Cho, M. *Int. J. Quantum Chem.* **2005,** *104,* 616.

(50) Fang, C.; Wang, J.; Kim, Y. S.; Charnley, A. K.; Barber-Armstrong, W.; Smith, A. B., III; Decatur, S. M.; Hochstrasser, R. M. *J. Phys. Chem. B* **2004,** *108,* 10415.

(51) DeFlores, L. P.; Ganim, Z.; Nicodemus, R. A.; Tokmakoff, A. *J. Am. Chem. Soc.* **2009,** *131,* 3385.

(52) Fang, C.; Hochstrasser, R. M. *J. Phys. Chem. B* **2005,** *109,* 18652.

(53) Mukherjee, P.; Kass, I.; Arkin, I. T.; Zanni, M. T. *J. Phys. Chem. B* **2006,** *110,* 24740.

(54) Woutersen, S.; Hamm, P. *J. Chem. Phys.* **2001,** *115,* 7737.

(55) Backus, E. H. G.; Nguyen, P. H.; Botan, V.; Pfister, R.; Moretto, A.; Crisma, M.; Toniolo, C.; Stock, G.; Hamm, P. *J. Phys. Chem. B* **2008,** *112,* 9091.

(56) Roy, S.; Jansen, T. L. C.; Knoester, J. *Phys. Chem. Chem. Phys.* **2010,** *12,* 9347.

(57) Hasegawa, T.; Tanimura, Y. *J. Chem. Phys.* **2008,** *128,* 064511.

(58) May, V.; Kühn, O. *Charge and Energy Transfer Dynamics in Molecular Systems*; Wiley: Berlin, Germany, 2000.